Targeting the T-Cell Lymphoma Epigenome Induces Cell Death, Cancer Testes Antigens, Immune-Modulatory Signaling Pathways

Luigi Scotto[1,2], Cristina Kinahan[1,2], Eugene Douglass[3], Changchun Deng[1,2], Maryam Safari[4], Beatrice Casadei[1,2], Enrica Marchi[1,2], Jennifer K. Lue[1,2], Francesca Montanari[1,2], Lorenzo Falchi[1,2], Changhong Qiao[5], Nandakumar Renu[5], Susan E. Bates[4], Andrea Califano[3,7,8,9,10,11], and Owen A. O'Connor[6]

ABSTRACT

The peripheral T-cell lymphomas (PTCL) could be considered the prototypical epigenetic disease. As a disease, they are uniquely sensitive to histone deacetylase (HDAC) and DNA methyltransferase (DNMT) inhibitors, both alone and in combination, are characterized by a host of mutations in epigenetic genes, and can develop spontaneously in genetically engineered murine models predicated on established recurring mutations in (*RHOAG17V*) and *TET2*, an epigenetic gene governing DNA methylation. Given the clinical benefit of HDAC inhibitors (HDACi) and hypomethlyation agents alone and in combination in PTCL, we sought to explore a mechanistic basis for these agents in PTCL. Herein, we reveal profound class synergy between HDAC and DNMT inhibitors in PTCL, and that the combination induces degrees of gene expression that are substantially different and more extensive than that observed for the single agents. A prominent signature of the combination relates to the transcriptional induction of cancer testis antigens and genes involved in the immune response. Interestingly, *TBX21* and *STAT4*, master regulators of TH1 differentiation, were among the genes upregulated by the combination, suggesting the induction of a TH1-like phenotype. Moreover, suppression of genes involved in cholesterol metabolism and the matrisome were also identified. We believe that these data provide a strong rationale for clinical studies, and future combinations leveraging an immunoepigenetic platform.

Introduction

The peripheral T-cell lymphomas (PTCL) are a rare and heterogeneous group of non-Hodgkin lymphomas (NHL) associated with a poor prognosis (1), as only 15%–25% of patients can expect long-term survival following conventional chemotherapy. The median progression-free survival (PFS) and overall survival (OS) for patients in first relapse has been shown to be only 3.5 and 6 months, respectively (2). Emerging insights into the pathogenesis of PTCL, coupled with emerging preclinical and clinical experiences, have begun to suggest that the PTCL may be the prototypical epigenetic disease, an understanding that could create new opportunities to treat the disease.

For example, four histone deacetylase (HDAC) inhibitors [vorinostat, romidepsin (Romi), belinostat, and chidamide], have received regulatory approvals for patients with relapsed or refractory (R/R) PTCL around the world (3–6). These drugs exhibit clear class effects, producing an overall response rate (ORR) of about 25% to 30%, and a duration of response in excess of a year across a diversity of aggressive PTCL subtypes. Similarly, preliminary data have demonstrated that injectable azacitidine (AZA) produces an ORR of 52% [9 of 12 patients with angioimmunoblastic T-cell lymphoma (AITL), and 1 of 7 with PTCL-NOS] in a highly selected patient population (7). There is no other neoplastic disease for which HDAC inhibitors (HDACi) have demonstrated such consistent class effect, and no other cancer beyond myeloid malignancies that display this degree of vulnerability to DNMT inhibitors. Recurring mutations have been described previously in isocitrate dehydrogenase (*IDH2*), Ten-Eleven Translocation 2 (*TET2*), and DNA methyltransferase (*DNMT3A*), among patients with select subtypes of PTCL (8–10). These genes govern transcription through DNA methylation. These mutations, which appear to be more commonly found in select subtypes like AITL and PTCL-TFH, conspire to produce presumed genome-wide hypomethylation and transcriptional repression. In theory, hypomethylating agent (HMA) would be the pharmacologic counter-balance to the biological consequences of these mutations.

Another compelling line of evidence comes from genetically manipulated murine models predicated on *TET2* mutations. Using two distinctly different experimental approaches, Palomero and colleagues (9, 11) and Sakata and colleagues (12) demonstrated that mutations

[1]Center for Lymphoid Malignancies, Columbia University, Medical Center, New York, New York. [2]Division of Experimental Therapeutics, Columbia University, Medical Center, New York, New York. [3]Department of Systems Biology, Columbia University, New York, New York. [4]Division of Hematology and Oncology, Columbia University, Medical Center, New York, New York. [5]Department of Medicine, Biomarkers Core Laboratory, Columbia University, Medical Center, New York, New York. [6]Department of Medicine, University of Virginia, Charlottesville, Virginia. [7]Herbert Irving Comprehensive Cancer Center, Columbia University, New York, New York. [8]Department of Biomedical Informatics, Columbia University, New York, New York. [9]Department of Biochemistry and Molecular Biophysics, Columbia University, New York, New York. [10]Department of Medicine, Vagelos College of Physicians and Surgeons, Columbia University, New York, New York. [11]J.P. Sulzberger Columbia Genome Center, New York, New York.

Note: Supplementary data for this article are available at Molecular Cancer Therapeutics Online (http://mct.aacrjournals.org/).

Corresponding Author: Owen A. O'Connor, University of Virginia, 1240 Lee Street, Charlottesville, VA 22903. Phone: 917-992-5214; E-mail: owenaoconnor27@gmail.com

Mol Cancer Ther 2021;20:1422–30

doi: 10.1158/1535-7163.MCT-20-0377

in the Ras Homolog Family Member A (*RHOA)* small GTPase (*RHOA*G17V mutations) appear to cooperate with loss-of-function mutations in *TET2*, an epigenetic tumor-suppressor gene, to produce spontaneous AITL. In similar fashion, a novel *FYN–TRAF3IP2* fusion joining the N-terminal regulatory domains of *FYN* with *TRAF3IP2* has been identified as a recurrent driver of PTCL-NOS and AITL lymphomagenesis (13). Strikingly, retroviral expression of FYN–TRAF3IP2 in bone marrow progenitors cooperated with TET2 inactivation in CD4-positive cells to induce development of $CD4^+$ PTCL-NOS lymphoma in mice. Collectively, these mouse models establish that mutations in epigenetic drivers can cooperate with other commonly found mutations in PTCL to produce spontaneous PTCL. Recently, our group has pioneered the translational development of novel epigenetic predicated drug:drug combinations in PTCL, many of which have been validated in preclinical and clinical studies (14–17). A recent Phase I study of oral AZA plus Romi produced an ORR for the entire study population, the B-cell, and patients with PTCL of 37%, 11%, and 83% respectively, with CR occurring only among patients with PTCL. Among 8 evaluable patients with AITL, the ORR was 100% (18). In addition, after a median follow-up of 15.3 months, the PFS for the T-cell patients was not reached, versus only 2.5 months for patients with B-cell lymphoma (19).

Collectively, these data point to a driver role for epigenetic lesions in PTCL, and suggest an exquisite intrinsic sensitivity to epigenetic modifiers. Herein, we seek to elucidate the mechanistic basis for these epigenetic combinations in PTCL, and establish a logic for integrating complementary agents to reconfigure the front-line and beyond treatment for patients with PTCL.

Materials and Methods

Cell lines and culture

Cell lines were obtained from the ATCC, DSMZ (Braunschweig, Germany), Kyoto and Fukujima University (Japan). Authenticated and tested for *Mycoplasma* and cultured in RPMI-1640 medium with heat-inactivated 10% FBS.

Materials

All drugs were purchased from Selleckchem and dissolved in DMSO.

Cytotoxicity assays

Cells were seeded at a concentration of 5×10 (4) cells/mL (H9, P12, PF382, TLOM1, and MT2), 2.5×10 (4) cells/mL (C5MJ) or 1×10 (5) cells/mL (HH). Cell viability was assessed using the Cell Titer Glo assay (Promega), as previously described (20, 21). Synergy of the combinations was calculated using the Excess Over Bliss (EOB) methodology (22). Luminescence was detected using the multimode plate reader GloMax Discover system (Promega).

Western blotting

Western blotting was performed according to the standard protocols, using a chemiluminescence detection system (Thermo Scientific). The following primary antibodies included are: Anti-TBX21, anti-STAT4, anti–PD-L1, and anti–β-actin (Cell Signaling Technology), anti–MAGE-A1, anti-PRAME, anti-MVK, and anti-DHCR24 (Santa Cruz Biotechnology).

Methylation analysis

Genomic DNA was purified from cells using the salting out procedure and purified using the genomic DNA clean and concentrator Kit (Zymo Research). The content and purity of the collected RNAfree DNA was assessed on a Nanodrop 8000 spectrophotometer (Thermo Fisher Scientific). One μg of genomic DNA was digested in a 100 μL reaction mixture at 37°C for 6 hours and filtered using ultrafree centrifugal filters (Millipore). LC analysis was performed with an Agilent 6410 LC-MS/MS system. The percentage of methylation was calculated as: methylation percentage = [5mdC]/[dG], according to the calibration curve. Determination of the percentage of 5-methyl-2′-deoxycytidine (MdC) was performed using LC-tandem MS methods previously described (23). Internal standard were prepared as previously described (23). Calibration standards were prepared spanning a range of 0.1 ng/mL to 5 μg/mL and analyzed as previously described for the samples.

Gene expression profiling

Total RNA was extracted using RNeasy mini kit (Qiagen) from cells collected after 96 hours incubation with or without drugs. RNA quantitation and quality were assessed by the Agilent Bioanalyzer 2100. RNA libraries prepared from poly-A pull-down enrich mRNAs from total RNA samples (Illumina TruSeq RNA prep kit), and were sequenced at the Columbia Genome Center using Illumina HiSeq2500/HiSeq4000. DEseq software, an R package based on a negative binomial distribution that models the number reads from RNA-seq experiments and test for differential expression, was used to test for differentially expressed genes under various conditions. For visualization, raw counts were normalized sample-wise to reads per million (RPM) and differential expression was calculated for each cell-line as a z-score centered at untreated controls. Hierarchical clustering was calculated by euclidean distance using the hclust function in the stats R package and visualized using the heatmap.2 function within the gplots R package. Unclustered heat maps were also generated with the heatmap.2 function with samples organized by cell-line and drug concentrations and genes organized by pathway annotation. Principal component analysis was evaluated using prcomp function in the stats R package. In the matrix, each column represents a sample and each row represents a gene. The data discussed in this publication have been deposited in NCBI's Gene Expression Omnibus (GEO) and are accessible through GEO Series accession number GSE148069 (https://www.ncbi.nlm.nih.gov/geo/query/acc.cgi?acc = GSE148069).

RT-qPCR

RNA samples extracted for gene expression profiling were used to proceed with RT-qPCR analysis. cDNA was made using the Omisncript RT Kit (Qiagen). TaqMan Fast Advanced Master Mix and FAM-MGB primers were purchased from Thermo Fisher Scientific. Reactions were conducted on a StepOnePlus Real-Time PCR System (Applied Biosystem).

Conditioned-medium proliferation assay

Conditioned medium (CM) was collected from cells exposed or not exposed to Romi and sequential AZA. Isolated PBMCs 1.35×10 (5) were seeded in a 120 μL of growth medium composed of RPMI-1640/10% FCS (control), 1/3 of RPMI-1640/10% FCS and 2/3 of CM from untreated or Romi plus AZA-treated cells. For activation of T cells, Dynabeads human T-activator CD3/CD28 was used following the manufacturer's recommendations. Cell viability was assessed using the Cell Titer Glo assay (Promega), as previously described. PBMCs of three independent donors were used for the proliferation assay. The box and whisker plot displays the summary of data collected from no less than five determinations.

Results

Romi and AZA synergize in T-cell lymphoma cell lines

The deregulated gene expression observed during initiation and progression of cancer involves a complex interplay between the hypermethylation of CpG islands within gene promoters and the deacetylation/methylation of histone tails. Although HDACis are approved for patients with relapsed PTCL, single agent AZA has exhibited some activity in only select subtypes of the disease (7). The combination of HDACi and an HMA, invoking two distinctly different epigenetic mechanisms, appears to exhibit potent class synergy in preclinical models, with compelling clinical activity in patients with relapsed and refractory (R/R) PTCL (19). We validated this class synergy on cell viability across a panel of 6 T-cell lymphoma (TCL) cell lines exposed to various combinations of AZA, decitabine, Romi, and belinostat (**Fig. 1A** and **B**, Supplementary Figs. S4 and S5). Notably, the combination of AZA and Romi demonstrated potent synergy as assessed by the EOB methodology. HMAs function through their incorporation into DNA (decitabine more than AZA) and RNA (AZA). By being incorporated into the DNA, HMAs form a covalent bond with DNMTs leading to degradation of DNMT with the resultant inhibition of methylation. To clarify the effect of the incorporation of AZA into DNA, methylation of cytosine residues was evaluated using mass spectrometry in 6 TCL cell lines following exposure to various concentrations of AZA. The effect of AZA incorporation into DNA, evaluated as the percentage of methylated cytosine (%MdC) of hyrdrolyzed genomic DNA, revealed a 50%–70% decrease in MdC in all six T-cell lines when compared with untreated controls (**Fig. 1C**). Exposure to Romi alone produced no effect on DNA methylation, and in combination with AZA did not impact DNA demethylation differently from AZA alone (Supplementary Fig. S1). These data establish that the observed demethylation in the combination was solely due to the AZA exposure.

The combination of AZA and Romi leads to a unique genetic signature

To determine the differential effects of AZA, Romi, and the combination on gene expression as a means to gain mechanistic insight, we exposed 4 TCL cell lines (H9, HH, TLOm1, and PF382) to a 96-hour treatment to single-agent AZA (sequential daily administration × 96 hours), Romi (single pulse dose on day 1) or the combination of AZA-Romi (given as noted for the single agents). Given the short half-life of AZA in cell culture (<8 hour) and the restricted cell-cycle window for DNA incorporation (S-phase), AZA was administered on a daily schedule.

Following single-agent exposure to Romi and AZA, unsupervised gene expression profile (GEP) analysis revealed that 38 and 409 unique

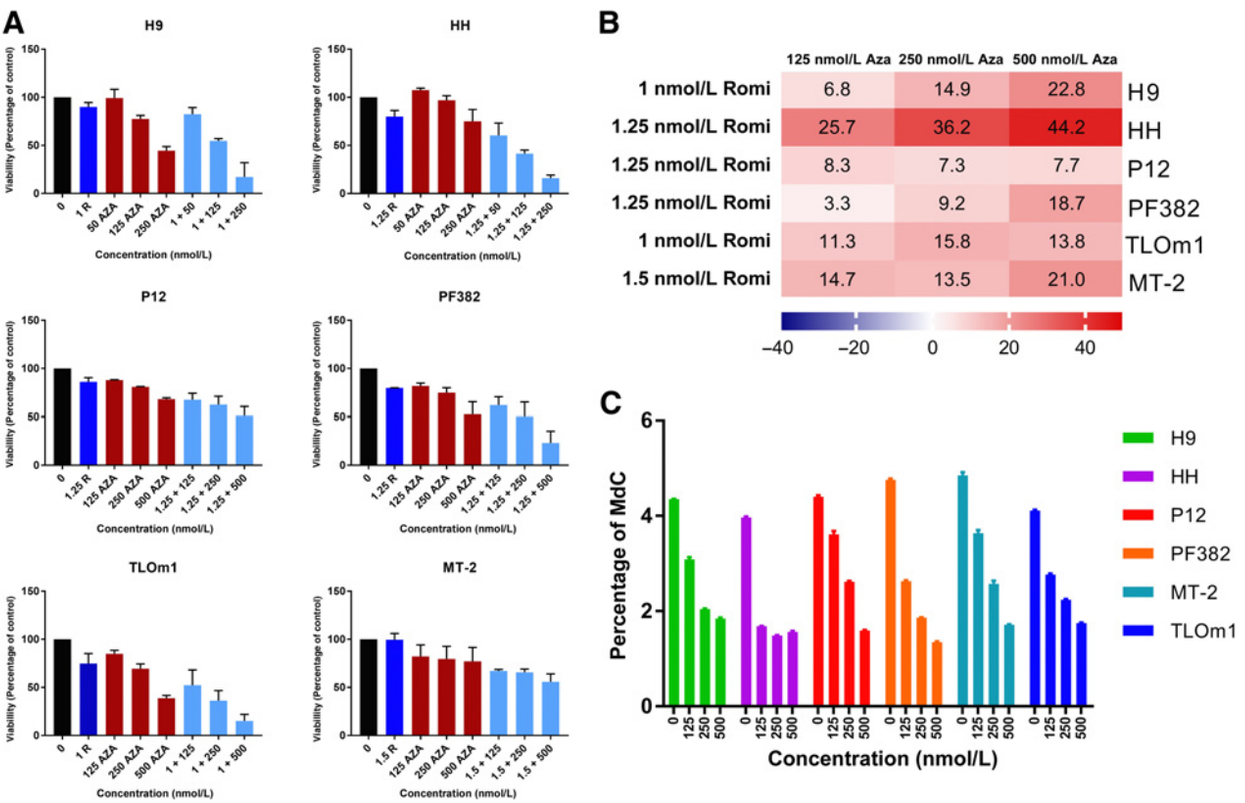

Figure 1.

Synergistic activity of Romi and AZA in T-cell lymphoma lines. **A,** Synergistic cytotoxic activity of Romi (R) and sequential AZA combination was evaluated on a panel of six T-cell lymphoma lines, using IC (10–20) of R and increased AZA concentration (50, 125, 250 nmol/L). Drug:drug interaction was evaluated at 96 hours from first addition. **B,** EOB values represent average measurements of synergy of three independent experiments. **C,** DNA hypomethylation measured as the percentage of MdC in the six T-cell lymphoma lines exposed to sequential AZA exposure. Error bars represent standard deviation of three or more separated experiments.

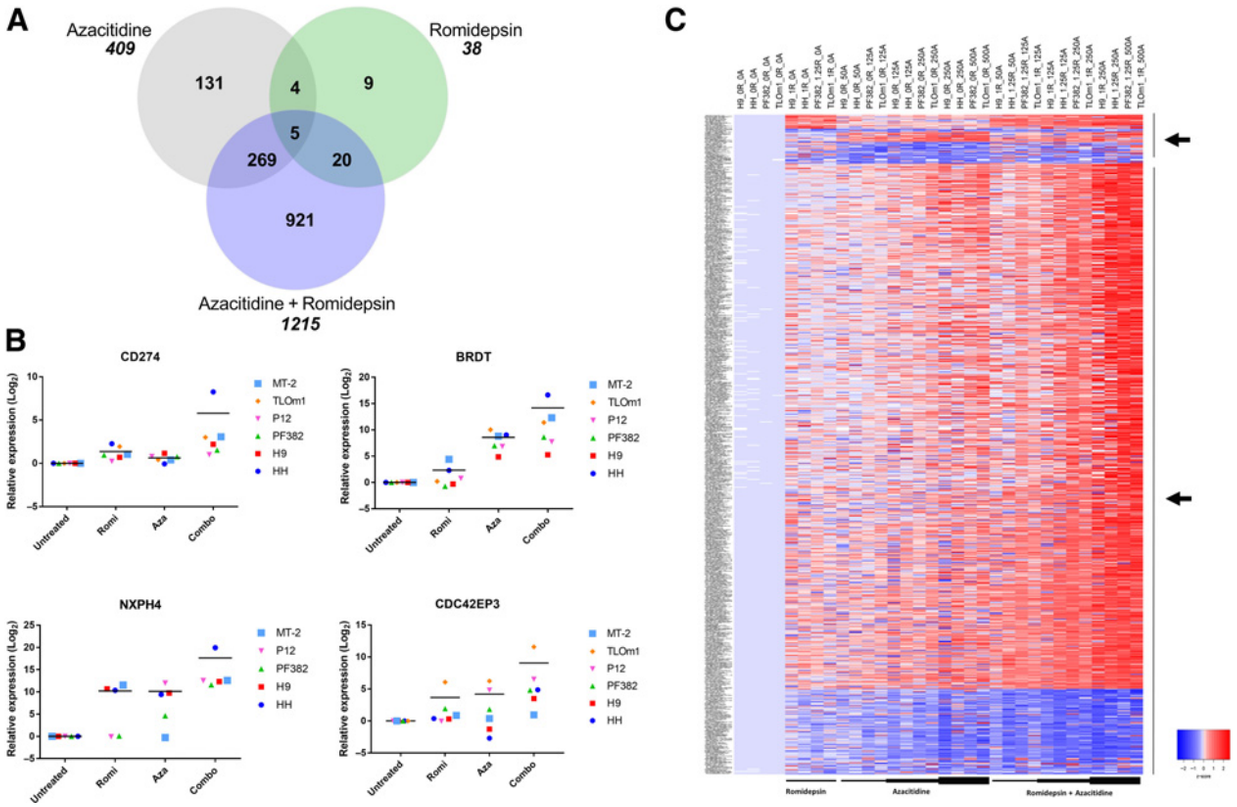

Figure 2.

The Romi plus AZA combination modulates a unique set of genes. **A,** The Venn diagram shows the relationship among genes included in the three signatures (adjusted *P* value ≤0.05). The expression of 921 genes is uniquely modulated by the combination treatment. Number of genes modulated by each treatment are also shown. **B,** Confirmation of GEP data by quantitative RT-PCR. The differential expression of four selected genes (*CD274, BRDT, NXPH4*, and *CDC42EP3*) was analyzed in control and treatment groups in a panel of T-cell lymphoma lines to validate GEP signatures. The qPCR results were normalized using β-actin. qPCR data represent the mean of three determinations and express as Log_2 fold change with respect to control. Horizontal bars represent the grand mean among all cell lines. **C,** Supervised analysis of gene expression in TCL lines based on the expression of genes modulated by single agent and combination (adjusted *P* value 0.05, Log_2 fold change absolute value 0.5). Arrows indicated gene sets uniquely modulated by the two single agents (top arrow) and combination (bottom arrow).

genes were modulated, respectively, whereas 1,125 genes were modulated following exposure to the combination of AZA-Romi (**Fig. 2A**, Supplementary Fig. S2). The vast majority (269/409 and 20/38) of the genes modulated by the single agents were similarly modulated by the combination. However, the combination induced a markedly more significant change in the transcriptome, as an additional 921 genes were uniquely altered after exposure to the AZA–Romi combination. Using supervised GEP, where modulated genes were defined by adjusted *P* value of 0.05, log_2 fold change >0.5, exposure to AZA–Romi induced a significant increase in the number of genes modified by the combination compared with either single agent alone (**Fig. 2C**). Moreover, a consistent modification of gene expression mirrored the increase in AZA concentration, indicating incremental demethylation, potentially resulting in augmented chromatin and promoter accessibility of previously silenced genes.

Validation of the GEP analysis was performed by RT-qPCR using 4 selected genes (*CD274, CDC42EP3, BRDT*, and *NXPH4*) in a panel of 6 TCL lines (H9, HH, PF382, TLOm1, P12, and MT-2; **Fig. 2B**). These genes were selected as they represent mechanisms of immune evasion (*CD274* aka *PDL1*), cytoskeleton regulation (*CDC42EP3*), cancer testis antigen (CTA) expression (BRDT) and signaling molecule (*NXPH4*). The modulation of gene expression by the single agents and combination was confirmed by the RT-qPCR data. The combination of AZA–Romi led to significant upregulation of the 4 probed genes compared with untreated samples.

Using gene set enrichment analysis, 2 major pathways emerged following exposure to the AZA–Romi combination: (i) matrisome-related genes such as proteins of the extracellular matrix (ECM) and ECM-associated proteins; and (ii) cholesterol biosynthesis regulation (**Fig. 3A**, Supplementary Fig. S3). Modulation of gene expression within the aforementioned pathways correlated with the degree of demethylation in response to the AZA–Romi treatment, suggesting an increase in transcriptional activation. The expression of several ECM core (26) and ECM-associated (54) proteins that define the matrisome was positively modulated by the combination treatment. In particular, within the matrisome, the expression of genes either coding for structural proteins such as *COL1A1, COL2A1, COL5A1, FN1, LAMA5*, or genes involved in ECM degradation such as *MMP17, ADAM11, ADAMTS14* or *ADAMTS20* were upregulated uniquely by combination treatment. Furthermore, the expression of genes encoding ECM-associated proteins that are not part of the matrisome but are nonetheless important in ECM remodeling such as growth factors, including *EGFL6, FGF14, VEGFC*, cytokines like *CSF3, IL18, CCL25*, and semaphorins like *SEMA6B*, was also modulated.

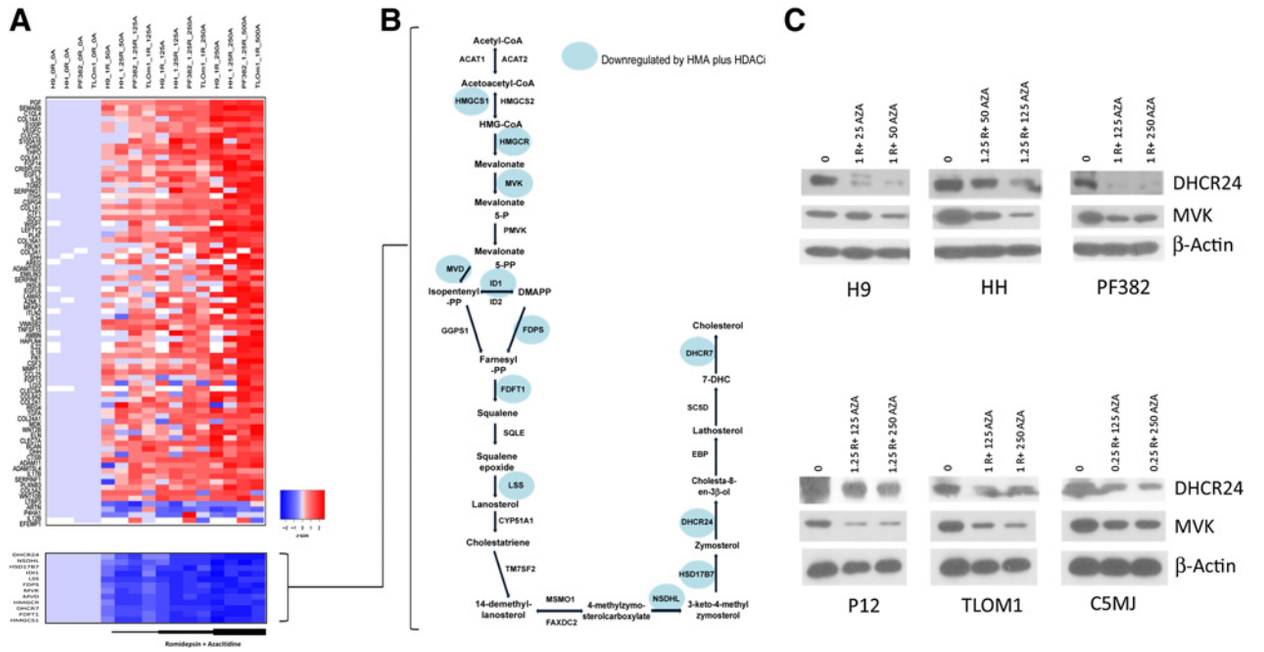

Figure 3

Matrisome perturbation and cholesterol biosynthesis downregulation in TCL as result of exposure to Romi plus AZA. **A,** Gene set enrichment analysis of genes modulated by the combinational therapy in TCL lines identify affected biological pathways associated with the matrisome and cholesterol biosynthesis. Each column represents a sample and correspondent treatment, each row represents a gene. Samples are grouped on the basis of treatment (from left to right: untreated, Romi, AZA and combination. **B,** The Cholesterol biosynthesis pathway. Highlighted in blue the 12 genes whose expression is downregulated by exposure to the combination. **C,** Western blot analysis of MVK and DHCR24 expression in TCLs exposed to drug–drug combination.

Downregulation of genes involved in cholesterol biosynthesis was observed in the single agent and combination-treated samples. Interestingly, enhanced inhibition was noted in the cell lines treated with AZA–Romi (**Fig. 3A**). Twelve genes were found to be substantially downregulated following exposure to the combination in six TCL cell lines (**Fig. 3A** and **B**). Among the downregulated genes were those involved in cholesterol synthesis, including *HMGCR* (rate limiting enzyme), *FDFT1, LSS* (catalyzes first step in the pathway), *DHCR7* (catalyzes last step), *MVD, MVK, FDPS, ID11* and *NSDHL*. Decreased protein expression of MVK and DHCR24 was confirmed in 6 TCL lines exposed to the combination (**Fig. 3C**). Taken together, the inhibitory impact of AZA-Romi on cholesterol biosynthesis suggests that potential cholesterol depletion can impair cell membrane integrity leading to apoptosis, which has been previously reported in diffuse large B-cell lymphoma (DLBCL) (24).

CTAs, immune and viral/IFN response genes are prominently induced after dual exposure to AZA and Romi

There is evidence suggesting that exposure to AZA increases the expression of various CTAs in a variety of *in vitro* and *in vivo* tumor models (25–27). Although exposure to Romi did not induce the expression of any CTAs, exposure to AZA induced the expression of 21 CTA genes, albeit to a modest extent in 4 TCL cell lines (**Fig. 4A** and **B**). However, the combination of AZA–Romi modulated the expression of a broader number of CTA genes ($n = 38$), and augmented the expression of the 21 AZA-induced genes by approximately a log fold (**Fig. 4B**). Thus, dual inhibition of HDACs and DNMT not only augmented the level of expression of the 21 CTAs induced by AZA alone, but also diversified and increased the repertoire of CTA expression.

Notably, among the CTA genes whose expression was enhanced by co-exposure to AZA–Romi were *MAGE-A1* and *PRAME. MAGE-A1* was the first CTA identified on the basis of its ability to induce an autologous cytotoxic T-lymphocyte response (28), whereas *PRAME* has been found to be expressed in a variety of malignant tumors and is a potential candidate for cancer immunotherapy (29). The AZA–Romi combination increased *MAGE-A1* and *PRAME* at both the RNA and protein level as confirmed by GEP and western blot analysis (**Fig. 4A–C**).

In addition, transcriptional upregulation of genes involved in the IFN response to viral infection (*PD-L1, IRF7, IL-18,* and *IFI6*) and innate/immune response (*IL22, IL26,* and *IL1R1*) was also observed across all four cell lines exposed to the combination treatment relative to control (**Fig. 4A**). The expression of *PD-L1* (*CD274*), a target of immune checkpoint therapy, was upregulated by exposure to Romi and enhanced by the combination treatment (**Fig. 4B**). Intriguingly, the other INF/viral and immune-related genes were only induced by the combination of AZA-Romi and not by the single agents (**Fig. 4B**).

In concert with *STAT4, TBX21* (T-bet) has been shown to play a central role in the generation of transcriptionally competent TH1 cell-specific genes in CD4-positive T cells (30). The transcriptional expression of these two genes was induced after dual exposure to HDAC and DNMT inhibitors, which was confirmed by western blot analysis (**Fig. 4A–C**). The collective effects of AZA–Romi exposure can potentially contribute to the development of a TH1 microenvironment supported by pro-inflammatory cytokines, in turn facilitating recruitment of leukocytes and stimulation of CD4-positive T-cell activation and proliferation.

To assess whether the AZA–Romi combination imparted any impacts on TH1 polarization, supernatants from four cell lines (H9,

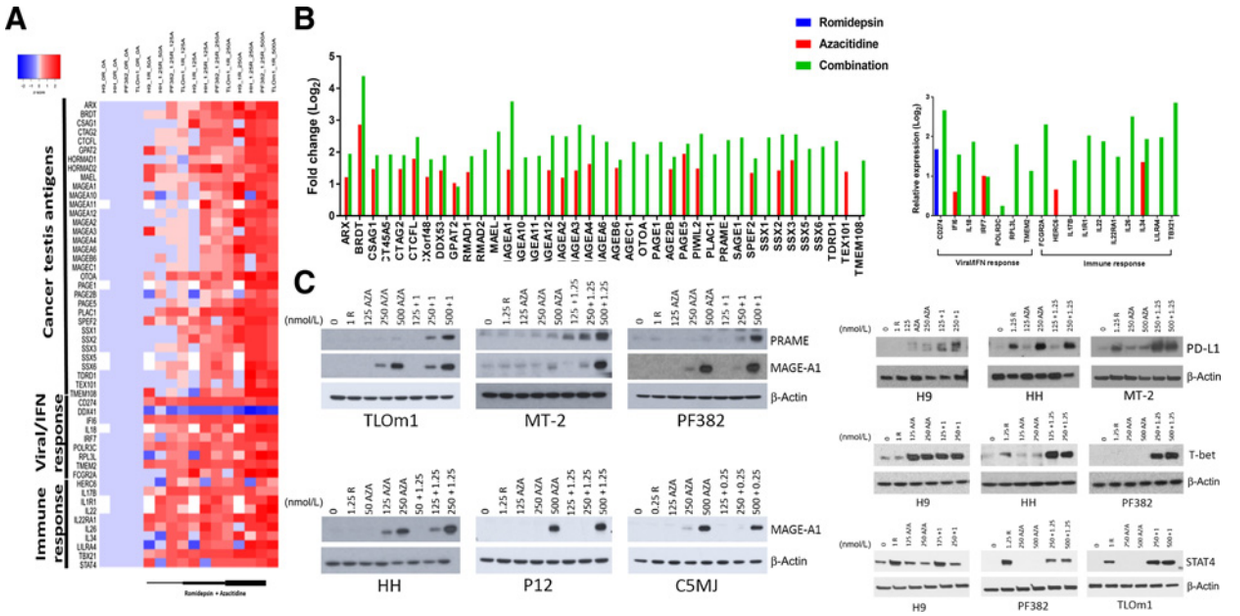

Figure 4.

Upregulated expression of the cancer testis antigens and immune response genes in TCL by the Romi and AZA combination. **A,** Supervised analysis in TCL lines based on the expression of cancer testis antigens and immune response genes modulated by the combinational therapy. **B,** Cancer testis antigens (CTA) and immune response genes increased mRNA levels in T-cell lymphoma lines as result of Romi and AZA treatment. **C,** MAGE-A1, PRAME, STAT4, TBX21, and PD-L1 protein levels in T-cell lymphoma lines exposed to single agent and combination. Romi (R), azactidine (AZA).

HH, PF382, and TLOM1) exposed to the AZA–Romi combination were assayed for their proliferative properties on healthy donor PBMCs. As shown in **Fig. 5A**, the activated T-lymphocytes of healthy donors grown in the presence of CM collected from TCL cells exposed to the AZA–Romi treatment provided a proliferative advantage over activated T-lymphocytes grown in the presence of CM of untreated TCL cells. Moreover, TH subset characterization indicates a preferential increase in the TH1 population when PBMC grown in CM of treated cells where compared with PBMC grown in CM of untreated cells (**Fig. 5B**). Therefore, on the basis of these data, it is likely that the AZA–Romi combination has an important impact on the tumor–immune microenvironment by promoting the stimulation of activated T-lymphocytes, and theoretically mitigating against a tumor evasion profile.

Discussion

AZA and decitabine represent one of two classes of epigenetic-based drugs used in cancer therapy (31). These DNMT inhibitors are only FDA approved for the treatment of acute myelogenous leukemia and

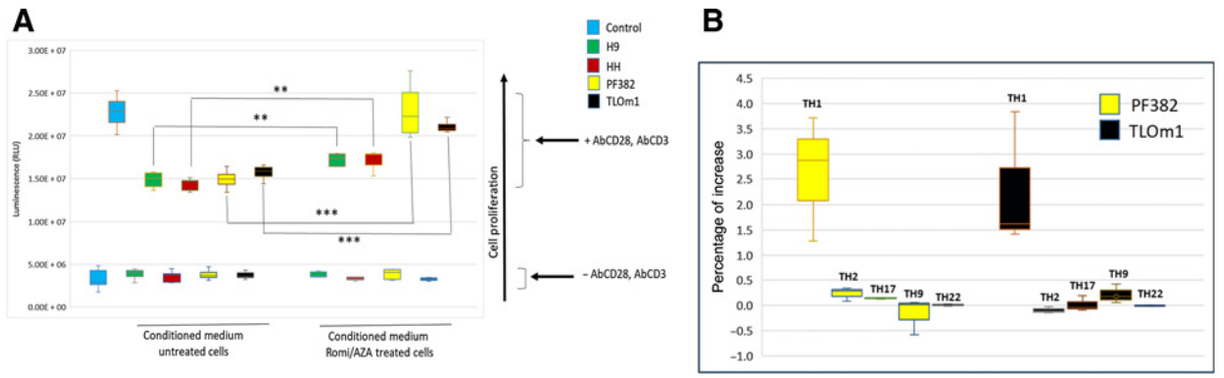

Figure 5.

Proliferative effect of conditioned medium on PBMC and TH phenotype characterization. **A,** Arrows indicate samples grown in absence or presence of CD3/CD28 dynabeads. Number of viable cells was determined on the basis of quantitation of ATP using luminescent cell viability assay. PBMCs of three independent donors were used for the proliferation assay. **B,** TH phenotype characterization of PBMCs. Increase percentile (treated/untreated) of TH subtypes in PBMC using CMs from PF382 and TLOM1 cell lines. The box and whisker plot displays the summary of data collected from no less than five determinations. **, $P \leq 0.01$; ***, $P \leq 0.001$.

myelodysplastic syndromes (32). Although there is only a modest experience with these drugs in lymphoma, they are typically not recognized as active across the spectrum of other malignant diseases, let alone NHL. In contrast, HDACis carry single-agent approval only in PTCL, demonstrating limited to no activity across other forms of cancer, including B-cell lymphoma and Hodgkin lymphoma (3, 4, 6). Although there are at best scant data on the combination of these drugs in lymphoma, several studies have and continue to explore these combinations in various solid-tumor malignancies, mostly as a strategy to improve tumor immunogenicity and host immune response (33). Interestingly, neither of these classes of drugs, as single agents or in combination, have been reported to demonstrate any activity in solid-tumor malignancies (34, 35). In PTCL, preclinical and clinical data have begun to firmly establish that combinations of DNMT and HDACis are potently synergistic, especially in AITL and likely the PTCL-TFH subtypes (15). Although many malignant diseases carry a host of mutations in epigenetic genes, it is unclear whether these genetic aberrations predispose the cell to increased vulnerability to one type of epigenetic modifiers or not. Taken together, multiple lines of data have begun to distinguish the PTCL as the one neoplastic disease that appears to exhibit a unique and marked vulnerability to epigenetic modifiers.

Similar to what was reported first by Marchi and colleagues (15) and subsequently by Rozati and colleagues (36), there appears to be class synergy between DNMT and HDACis in T-cell malignancies, seemingly at a level not previously seen for any other malignant disease. Partial insights into the mechanistic basis for this synergy can be derived from the GEP data. We demonstrate a unique alteration in the genetic signature of TCL cells exposed to the combination of AZA–Romi. Interestingly, the number of genes perturbed by the combination is substantially greater than that observed with the single agents, suggesting that the synergy is likely secondary to those distinctly perturbed genes. Moreover, these genes appear to fall into four broad categories, including those related to the: (i) matrisome/ECM regulation; (ii) cholesterol biosynthesis; (iii) CTAs; and (iv) viral/INF immune-related responses.

The gene expression alterations noted in the matrisome/ECM and cholesterol biosynthesis have translational implication. The ECM is a complex scaffolding structure that not only functions as an anchorage for surrounding cells, but can also influence cellular behavior, including cell proliferation, apoptosis, and migration (37, 38). In fact, increased ECM content has been associated with inferior prognosis and aggressive biology in colon cancer and breast cancer (39, 40). Here, we demonstrated that genes involved in ECM degradation such as *MMP17, ADAM11*, and *ADAMTS14*, were upregulated by the combination treatment. Thus, the impact on the matrisome and its ECM proteins in our experiments potentially suggests a role for re-modeling of the tumor microenvironment after exposure to AZA–Romi. The importance of the tumor microenvironment has been recently established in AITL, where differences in the microenvironment can have prognostic import. This emphasizes the need for more intensive correlative studies in future clinical trials investigating immunoepigenetic platforms (41). Similarly, impairing cellular cholesterol metabolism in DLBCL has been shown to induce apoptosis, albeit the precise mechanism remains to be defined (24).

Another set of genes markedly altered by the combination includes those in the family of CTAs and the IFN signaling pathway. The patterns of change in the CTA reveal that Romi alone has little to no impact on the expression of these genes, save the noted increase in *PD-L1*. Recent data suggest that this may be mediated specifically by HDAC3 (34). In contrast, single-agent AZA induced a broad spectrum of CTAs at a modest level, whereas, surprisingly, the combination of AZA–Romi increased both the spectrum and intensity of CTAs as well as genes in the IFN pathway. Although these findings likely do not explain the *in vitro* synergy, they may have important ramifications in patients. The immunological influences of the combination are underscored by the induction of genes involved in the IFN signaling pathway, providing at the least, a theoretical capacity to elicit a cancer-specific immune response. In this context, the induced expression of STAT4 and TBX21 may play an important role in the expression of secreted proteins that could induce recruitment and proliferation of activated T cells. Intriguingly, in patients with PTCL-NOS, TBX21 expression has shown to be associated with a more favorable prognosis compared with patients with a GATA3 expression (41), though there has been no mechanistic rationale to explain why this is the case. Validating these observations in patients is a crucial and integral feature of our ongoing clinical studies.

In addition to the induction of apoptosis in the tumor cells proper, the induction of CTA, IFN signaling, immune response genes, expression of TH-1–driven cytokines, and changes in STAT-4, point toward an immunological-mediated mechanism for the AZA–Romi combination, one that will need to be interrogated more thoroughly in the clinical setting. The induced expression of PD-L1 by Romi, which is maintained and increased upon with the addition of AZA, raises the interesting prospect that checkpoint inhibitors could represent one rational drug to integrate into the doublet. In fact, we have recently launched two clinical studies (NCT03240211 and NCT03161223) exploring the integration of a PD-1 (pembroluzimab) and PD-L1 inhibitors (durvalumab) with various epigenetic-based combinations in PTCL. Although the marked induction of CTAs by the combination may further augment the impact of the checkpoint inhibitor, it also raises the prospect that vaccines against these CTAs could represent yet another strategy to exploit the underlying mechanisms induced by the combined epigenetic modifiers.

Unfortunately, there are limited collections of cell lines representing the T-cell lymphomas. In fact, the 2 most common subtypes of PTCL, namely PTCL-NOS and AITL, are not represented in any collection to date. Our study has found that the distribution of mutations in genes like *IDH2, TET2*, and *DNMT3A*, is not present in most of the available T-cell lymphoma cell lines, presenting a challenge in describing any cause and effect relationship between the presence of a specific epigenetic mutation or collection of mutations, and their impact on their vulnerability to an epigenetic modifier. It is likely that our understanding regarding the import of these mutations will rely on data obtained from our ongoing T-cell lymphoma clinical trials where RNAseq is being used to appreciate the impact of the mutational landscape on drug activity. Moreover, using planned RNA-seq in these trials, we will also have the capability of validating the preclinical GEP findings described in this article.

Albeit early, there is mounting evidence that the PTCL may be particularly vulnerable to epigenetic modifiers, especially in combination. These data suggest that the drugs may have two distinct mechanisms for producing an antitumor response. One based on the cytotoxic effects of the drugs, as supported by standard cytotoxicity data and the induction of apoptosis; and one based on an immunological mechanism of action. The later mechanisms will require detailed interrogation in clinical studies to decipher more thoroughly. Additional studies will continue to focus on identifying the strongest rationale for integrating complementary and

synergistic drugs onto a possible HDAC and DNMT inhibitor backbone. These agents may include exploring the merits of adding PI3k inhibitors, checkpoint inhibitor (PD-1, PDL-1, and CTLA-4), pralatrexate, and other classes of epigenetic modifiers like EZH2 inhibitors. It is likely that targeting the basal level of epigenetic dysregulation in PTCL, and coupling it with rational agents based on the mechanistic effects, will create a plethora of new upfront and relapsed treatment regimens.

Authors' Disclosures

E. Marchi reports grants from Celgene/BMS during the conduct of the study; as well as grants from Merck, other from Myeloid Therapeutics, personal fees from Kymera, and grants from Astex Therapeutics outside the submitted work. J.K. Lue reports grants and other from Kymera Therapeutics, as well as other from AstraZeneca, Astex Pharmaceuticals, Daiichi Sankyo, and Kura Oncology outside the submitted work. L. Falchi reports other from Hofmann-La Roche, and personal fees and other from GenMab outside the submitted work. S.E. Bates reports a patent for US9259452B2 issued to Celgene Corp and a patent for US8673888B2 issued to Astellas Pharma Inc. and US Department of Health and Human Services. Dr. Califano is founder, equity holder, and consultant of DarwinHealth Inc., a company that has licensed some of the algorithms used in this manuscript from Columbia University. Columbia University is also an equity holder in DarwinHealth Inc. O.A. O'Connor reports grants and personal fees from Celgene/BMS during the conduct of the study. No disclosures were reported by the other authors.

Authors' Contributions

L. Scotto: Conceptualization, data curation, formal analysis, supervision, validation, investigation, methodology, writing–original draft, writing–review and editing. **C. Kinahan:** Data curation, investigation, methodology. **E. Douglass:** Software. **C. Deng:** writing–review and editing. **M. Safari:** Data curation, investigation. **B. Casadei:** Data curation, investigation. **E. Marchi:** Writing–original draft, writing–review and editing. **J.K. Lue:** Data curation, writing–original draft, writing–review and editing. **F. Montanari:** Writing–original draft, writing–review and editing. **L. Falchi:** Writing–review and editing. **C. Qiao:** Investigation, methodology. **N. Renu:** Writing–review and editing. **S.E. Bates:** Writing–review and editing. **A. Califano:** Writing–review and editing. **O.A. O'Connor:** Conceptualization, data curation, supervision, funding acquisition, investigation, writing–original draft, writing–review and editing.

Acknowledgments

We would like to acknowledge Celegene, The Lymphoma Research Fund of Columbia University and the Leukemia and Lymphoma Society for providing research support. This research was supported by the following NIH grants to Andrea Califano: R35 CA197745 (Outstanding Investigator Award); S10 OD012351 and S10 OD021764 (Shared Instrument Grants).

The costs of publication of this article were defrayed in part by the payment of page charges. This article must therefore be hereby marked *advertisement* in accordance with 18 U.S.C. Section 1734 solely to indicate this fact.

Received May 6, 2020; revised October 13, 2020; accepted June 7, 2021; published first June 9, 2021.

References

1. Swerdlow SH, Campo E, Pileri SA, Harris NL, Stein H, Siebert R, et al. The 2016 revision of the world health organization classification of lymphoid neoplasms. Blood 2016;127:2375–90.
2. Vose J, Armitage J, Weisenburger D, International T. International peripheral T-cell and natural killer/T-cell lymphoma study: pathology findings and clinical outcomes. J Clin Oncol 2008;26:4124–30.
3. Coiffier B, Pro B, Prince HM, Foss F, Sokol L, Greenwood M, et al. Results from a pivotal, open-label, phase II study of romidepsin in relapsed or refractory peripheral T-cell lymphoma after prior systemic therapy. J Clin Oncol 2012; 30:631–6.
4. O'Connor OA, Horwitz S, Masszi T, Van Hoof A, Brown P, Doorduijn J, et al. Belinostat in patients with relapsed or refractory peripheral t-cell lymphoma: results of the pivotal phase II belief (CLN-19) study. J Clin Oncol 2015;33: 2492–9.
5. Shi Y, Dong M, Hong X, Zhang W, Feng J, Zhu J, et al. Results from a multicenter, open-label, pivotal phase II study of chidamide in relapsed or refractory peripheral T-cell lymphoma. Ann Oncol 2015;26:1766–71.
6. Olsen EA, Kim YH, Kuzel TM, Pacheco TR, Foss FM, Parker S, et al. Phase IIb multicenter trial of vorinostat in patients with persistent, progressive, or treatment refractory cutaneous T-cell lymphoma. J Clin Oncol 2007;25: 3109–15.
7. Lemonnier F, Dupuis J, Sujobert P, Tournillhac O, Cheminant M, Sarkozy C, et al. Treatment with 5-azacytidine induces a sustained response in patients with angioimmunoblastic T-cell lymphoma. Blood 2018;132:2305–09.
8. Couronne L, Bastard C, Bernard OA. TET2 and DNMT3A mutations in human T-cell lymphoma. N Engl J Med 2012;366:95–6.
9. Palomero T, Couronné L, Khiabanian H, Kim M-Y, Ambesi-Impiombato A, Perez-Garcia A, et al. Recurrent mutations in epigenetic regulators, RHOA and FYN kinase in peripheral T-cell lymphomas. Nat Genet 2014;46:166–70.
10. Cairns RA, Iqbal J, Lemonnier F, Kucuk C, de Leval L, Jais J-P, et al. IDH2 mutations are frequent in angioimmunoblastic T-cell lymphoma. Blood 2012; 119:1901–3.
11. Cortes JR, Ambesi-Impiombato A, Couronné L, Quinn SA, Kim CS, da Silva Almeida AC, et al. RHOA G17V induces T follicular helper cell specification and promotes lymphomagenesis. Cancer Cell 2018;33:259–73.
12. Sakata-Yanagimoto M, Enami T, Yoshida K, Shiraishi Y, Ishii R, Miyake Y, et al. Somatic RHOA mutation in angioimmunoblastic T-cell lymphoma. Nat Genet 2014;46:171–5.
13. Scourzic L, Couronné L, Pedersen MT, Della Valle V, Diop M, Mylonas E, et al. DNMT3A(R882H) mutant and Tet2 inactivation cooperate in the deregulation of DNA methylation control to induce lymphoid malignancies in mice. Leukemia 2016;30:1388–98.
14. Jain S, Jirau-Serrano X, Zullo KM, Scotto L, Palermo CF, Sastra SA, et al. Preclinical pharmacologic evaluation of pralatrexate and romidepsin confirms potent synergy of the combination in a murine model of human T-cell lymphoma. Clin Cancer Res 2015;21:2096–106.
15. Marchi E, Zullo KM, Amengual JE, Kalac M, Bongero D, McIntosh CM, et al. The combination of hypomethylating agents and histone deacetylase inhibitors produce marked synergy in preclinical models of T-cell lymphoma. Br J Haematol 2015;171:215–26.
16. Zullo KM, Guo Y, Cooke L, Jirau-Serrano X, Mangone M, Scotto L, et al. Aurora a kinase inhibition selectively synergizes with histone deacetylase inhibitor through cytokinesis failure in T-cell lymphoma. Clin Cancer Res 2015;21: 4097–109.
17. Kalac M, Scotto L, Marchi E, Amengual J, Seshan VE, Bhagat G, et al. HDAC inhibitors and decitabine are highly synergistic and associated with unique gene-expression and epigenetic profiles in models of DLBCL. Blood 2011; 118:5506–16.
18. Falchi L, Lue JK, Amengual EJ, Sawas A, Deng C, Enrica Marchi E, et al. A Phase 1/2 study of oral 5-azacitidine and romidepsin in patients with lymphoid malignancies reveals promising activity in heavily pretreated peripheral T-cell lymphoma (PTCL). Blood 2017;130(Supplement 1):1515.
19. O'Connor OA, Falchi L, Lue JK, Marchi E, Kinahan C, Sawas A, et al. Oral 5-azacytidine and romidepsin exhibit marked activity in patients with PTCL: a multicenter phase 1 study. Blood 2019;134:1395–405.
20. Marchi E, Paoluzzi L, Scotto L, Seshan VE, Zain JM, Zinzani PL, et al. Pralatrexate is synergistic with the proteasome inhibitor bortezomib in *in vitro* and *in vivo* models of T-cell lymphoid malignancies. Clin Cancer Res 2010;16:3648–58.
21. Deng C, Lipstein M, Rodriguez R, Serrano XOJ, McIntosh C, Tsai W-Y, et al. The novel IKK2 inhibitor LY2409881 potently synergizes with histone deacetylase inhibitors in preclinical models of lymphoma through the downregulation of NF-kappaB. Clin Cancer Res 2015;21:134–45.
22. Goswami CP, Cheng L, Alexander PS, Singal A, Li L. A new drug combinatory effect prediction algorithm on the cancer cell based on gene expression and dose–response curve. CPT Pharmacometrics Syst Pharmacol 2015;4:e9.
23. Quinlivan EP, Gregory JF III. DNA methylation determination by liquid chromatography-tandem mass spectrometry using novel biosynthetic [U-15N]deoxycytidine and [U-15N]methyldeoxycytidine internal standards. Nucleic Acids Res 2008;36:e119.

24. Rink JS, Yang S, Cen O, Taxter T, McMahon KM, Misener S, et al. Rational targeting of cellular cholesterol in diffuse large B-cell lymphoma (DLBCL) enabled by functional lipoprotein nanoparticles: a therapeutic strategy dependent on cell of origin. Mol Pharm 2017;14:4042–51.
25. Coral S, Sigalotti L, Altomonte M, et al. 5-aza-2'-deoxycytidine-induced expression of functional cancer testis antigens in human renal cell carcinoma: immunotherapeutic implications. Clin Cancer Res 2002;8: 2690–5.
26. Coral S, Sigalotti L, Colizzi F, Spessotto A, Nardi G, Cortini E, et al. Phenotypic and functional changes of human melanoma xenografts induced by DNA hypomethylation: immunotherapeutic implications. J Cell Physiol 2006;207: 58–66.
27. Guo ZS, Hong JA, Irvine KR, Chen GA, Spiess PJ, Liu Y, et al. De novo induction of a cancer/testis antigen by 5-aza-2'-deoxycytidine augments adoptive immunotherapy in a murine tumor model. Cancer Res 2006;66: 1105–13.
28. van der Bruggen P, Traversari C, Chomez P, Lurquin C, De Plaen E, Van den Eynde B, et al. A gene encoding an antigen recognized by cytolytic T lymphocytes on a human melanoma. Science 1991;254:1643–7.
29. Gutzmer R, Rivoltini L, Levchenko E, Testori A, Utikal J, Ascierto PA, et al. Safety and immunogenicity of the PRAME cancer immunotherapeutic in metastatic melanoma: results of a phase I dose escalation study. ESMO Open 2016;1: e000068.
30. Lazarevic V, Glimcher LH, Lord GM. T-bet: a bridge between innate and adaptive immunity. Nat Rev Immunol 2013;13:777–89.
31. Egger G, Liang G, Aparicio A, Jones PA. Epigenetics in human disease and prospects for epigenetic therapy. Nature 2004;429:457–63.
32. Gurion R, Vidal L, Gafter-Gvili A, Belnik Y, Yeshurun M, Raanani P, et al. 5-azacitidine prolongs overall survival in patients with myelodysplastic syndrome—a systematic review and meta-analysis. Haematologica 2010;95: 303–10.
33. Cohen AL, Ray A, Van Brocklin M, Burnett DM, Bowen RC, Dyess DL, et al. A phase I trial of azacitidine and nanoparticle albumin bound paclitaxel in patients with advanced or metastatic solid tumors. Oncotarget 2017;8:52413–19.
34. Booth L, Roberts JL, Poklepovic A, Kirkwood J, Dent P. HDAC inhibitors enhance the immunotherapy response of melanoma cells. Oncotarget 2017;8: 83155–70.
35. Juo Y-Y, Gong X-J, Mishra A, Cui X, Baylin SB, Azad NS, et al. Epigenetic therapy for solid tumors: from bench science to clinical trials. Epigenomics 2015;7:215–35.
36. Rozati S, Cheng PF, Widmer DS, Fujii K, Levesque MP, Dummer R. Romidepsin and azacitidine synergize in their epigenetic modulatory effects to induce apoptosis in CTCL. Clin Cancer Res 2016;22:2020–31.
37. Daley WP, Peters SB, Larsen M. Extracellular matrix dynamics in development and regenerative medicine. J Cell Sci 2008;121:255–64.
38. Boyd DF, Thomas PG. Towards integrating extracellular matrix and immunological pathways. Cytokine 2017;98:79–86.
39. Ahn S, Cho J, Sung J, Lee JE, Nam SJ, Kim K-M, et al. The prognostic significance of tumor-associated stroma in invasive breast carcinoma. Tumour Biol 2012;33: 1573–80.
40. Huijbers A, Tollenaar RAEM, v Pelt GW, Zeestraten ECM, Dutton S, McConkey CC, et al. The proportion of tumor-stroma as a strong prognosticator for stage II and III colon cancer patients: validation in the VICTOR trial. Ann Oncol 2013; 24:179–85.
41. Iqbal J, Wright G, Wang C, Rosenwald A, Gascoyne RD, Weisenburger DD, et al. Gene expression signatures delineate biological and prognostic subgroups in peripheral T-cell lymphoma. Blood 2014;123:2915–23.